ATLAS Pixel Radiation Monitoring with HVPP4 System

Igor Gorelov, Martin Hoeferkamp, Sally Seidel, Konstantin Toms
Department of Physics and Astronomy, University of New Mexico, Albuquerque, NM 87131, USA

In this talk we present the basis for the protocol for radiation monitoring of the ATLAS Pixel Sensors. The monitoring is based on a current measurement system, HVPP4. The status on the ATLAS HVPP4 system development is also presented.

1. Introduction

The High Voltage Patch Panel 4 (HVPP4) is a hardware system to connect and distribute and control the bias voltages to pixel sensors. In this note we describe the extension of HVPP4 system to measure, digitize, and control the currents drawn by the pixel sensors comprising the ATLAS Pixel Detector. The HVPP4 current measurement system will be monitoring the pixel sensor currents in situ and in real time without requirement of special runs. The design topology of the system under development is discussed in technical note [1]

The ATLAS Pixel Detector (see [2] [3] [4][5] and a talk at this conference [6]) comprises 1456 pixel modules in the Layer-0 (or B-Layer), Layer-1 and Layer-2 from the barrel area, 288 modules mounted on 3 discs in the forward area and another 3 discs in the backward area. The total number of modules is 1744 units. The geometry and module count for the barrel region of the pixel detector system are summarized in Table I. Modules are mounted on mechanical/cooling supports, called staves, in the barrel region. Thirteen modules are mounted on a stave and the stave layout is identical for all layers. The active length of each barrel stave is about 801 mm. The staves are mounted in half-shells manufactured from a carbon-fiber composite material. Two half-shells are joined to form each barrel layer. The two endcap regions are identical. Each is composed of three disk layers, and all disk layers are identical. The basic parameters of the endcap region are given in Table II. Modules are mounted on mechanical/cooling supports, called disk sectors. There are eight identical sectors in each disk.

The pixel sensor consists of a 256 ± 3 µm thick n-bulk. The bulk contains n^+ implants on the read-out side and the p-n junction on the back side. For each sensor tile, the 47232 pixel implants are arranged in 144 columns and 328 rows. In 128 columns (41984 or 88.9%) pixels have implant sizes of 382.5×30 µm^2 with a pitch corresponding to 400×50 µm^2, and in 16 columns (5248 or 11.1%) pixels have implant sizes of 582.5×30 µm^2 corresponding to a pitch of 600×50 µm^2. In each column eight pairs of pixel implants, located near the center lines, are ganged to a common read-out, resulting in 320 independent read-out rows or 46080 pixel read-out channels. This arrangement was chosen to allow for the connection of the sensor tile to 16 electronic front-end chips combined into a single module.

Table I Basic parameters for the barrel region of the ATLAS pixel detector system.

Layer Number	Mean Radius [mm]	Number of Modules	Number of Channels	Active Area [m^2]
0	50.5	286	13,178,880	0.28
1	88.5	494	22,763,520	0.49
2	122.5	676	31,150,080	0.67
Total		1456	67,092,480	1.45

Table II Basic parameters of the endcap region of the ATLAS pixel detector system.

Disk Number	Mean z [mm]	Number of Modules	Number of Channels	Active Area [m^2]
0	495	48	2,211,840	0.0475
1	580	48	2,211,840	0.0475
2	650	48	2,211,840	0.0475
Total one endcap		144	6,635,520	0.14
Total both endcaps		288	13,271,040	0.28

The sensitive area of ≈ 1.7 m^2 of the ATLAS pixel detector is covered with 1744 identical modules. Each module has an active surface of 6.08×1.64 cm^2.

We assume that the dominant radiation damage type is displacement defects in the bulk of the pixel sensor, caused by non-ionizing energy losses (NIEL). As the pixel barrel layers and disks are close to the interaction point the charged pions dominate the bulk damage. These defects increase the reverse leakage current, degrade the charge collection efficiency, and change the effective doping concentration which directly determines the depletion voltage. The leakage current strongly depends upon the temperature of the pixel sensor and the particle fluence through the sensor volume. We define the fluence $\Phi_{1MeV\,eq}$ as the number of particles causing damage equivalent to that of 1 MeV neutrons traversing 1 cm^2 of a sensor's surface. The ATLAS pixel detector integrated fluence

$\Phi_{1MeV\,eq}$, (measured in cm^{-2}), is expected to be proportional to integrated luminosity $\int L\,dt$, (measured in pb^{-1}).

The leakage current is monitored by the HVPP4 system at the pixel module granularity level. The bias voltage to the sensors is provided by voltage channels of power supply modules from Iseg [7]. During the first period of data taking, when the radiation damage of the sensors is small, 6 or 7 pixel modules will be fed by 1 Iseg power supply channel. At some level of radiation damage after inversion of the sensors, before the current drawn by 6 or 7 pixel modules will reach the Iseg limit, a number of power supplies will be added until the system provides 1 Iseg power supply channel per pair of pixel modules.

The current measurements on every module provide a powerful tool to monitor the status of every sensor, and hence the quality of the ATLAS Pixel Detector data. We will use the current measurements to estimate the fluence. We plan also to use the ad hoc ATLAS radiation monitoring devices [8] installed at several points of the pixel detector as well as the ones installed at other (outer) points of the ATLAS Inner Detector volume. That is, we will use two complementary data sets and methods to monitor the radiation in the ATLAS Pixel Detector physical volume.

As the bias current depends on the sensor temperature, temperature measurements and related data are of crucial importance. We will use the sensor temperature data from the temperature probes with which every module is equipped.

2. Leakage Current

The reverse bulk generation current's main cause is radiation damage of the crystal structure causing dislocations and other point defects.

Our analysis depends on the observation that increase in leakage current is proportional to fluence [9],

$$\Delta I = \alpha\,\Phi_{eq}\,V; \qquad (1)$$

where ΔI is the difference in leakage current at fluence Φ_{eq} relative to the value before irradiation of the physical volume V, and α is the current-related damage coefficient. The empirical parameter α has been measured [9] and found to be following:

$$\alpha(20^{\circ}C; 80min:@60^{\circ}C) = (3.99 \pm 0.03) \times 10^{-17}\,A/cm; \qquad (2)$$

at $20^{\circ}C$ after annealing for 80 minutes at $60^{\circ}C$.

When considering the linear ansatz described above we must add the caveat that the ansatz is applied to the leakage currents drawn by sensors past their beneficial annealing time periods. We expect that at the beginning of data taking and during beneficial annealing periods the sensors will be drawing the currents at the low level of dark currents before the irradiation damage takes its course. This fact stipulates the need of a sensitivity to a lowest range of pixel sensor leakage currents when the HVPP4 system will be particularly useful as an excellent debugging tool.

- We analyze $\Delta I/V$ (A/cm^3) vs $\int L\,dt$ (pb^{-1}) for each of the 1744 modules drawing current measured by the HVPP4 system.
- We assume that the fluence $\Phi_{1MeV\,eq}$ is proportional to the integrated luminosity $\int L\,dt$ and the fitted slope of $\Delta I/V$ vs $\int L\,dt$. Using the known α and the slope we will infer the fluence $\Phi_{1MeV\,eq}$ for each module.
- The current measurements are selected according to some quality criteria to be developed.
- The currents are corrected to a common temperature, $20^{\circ}C$ (still to be decided).

2.1. Lifetime Estimate

By comparing current with integrated luminosity we assume that the linear fits of the temperature-corrected current readings per module can be extrapolated to predict the amount of current the pixel modules will draw after a certain integrated luminosity has been collected with the ATLAS pixel detector.

Contrary to CDF SVX II, the ATLAS pixel S/N ratio is not an issue because the lowest noise level is determined by the sensor's design. However, leakage current in ATLAS Pixel Detector can lead to excessive power and thermal runaway, which basically limits the bias voltage that can be applied. A single Iseg power supply channel can sustain a maximum current of $I < 4000\,\mu A$ [7]. Initially we have 6 or 7 pixel modules biased by a single Iseg power supply channel what gives us a maximum current to be reached in the range of $I_{sensor} < (550...700)\,\mu A$.

Another important predictor of a pixel sensor's lifetime is its depletion voltage. We assume that the sensor will be kept biased at the full depletion voltage until limited by leakage current around 550 μA to 700 μA. After that the sensor will operate partially depleted with reduced signal amplitude resulting in reduced hit efficiency.

The next two periods of a pixel sensor's life should be expected:

- The first years, operated at full depletion. The end is determined by approaching
  - either a critical range of high currents with technically motivated cut-off values (we consider this case to be most probable),
  - or the maximum available bias voltage provided by the Iseg power supply at its channel level.

Later years of operation in partially depleted mode. At this point the sensor draws high current, still within the safety margin or at the maximum available bias voltage, but its pixels' hit efficiencies gradually diminish with integrated luminosity (or absorbed fluence).

2.2. ATLAS Radiation Field Measurements

The radiation field inside the ATLAS Inner Tracker volume is measured by a number of standard ATLAS radiation monitors [8]. We are interested in the devices sensitive to hadron NIEL radiation rather than ionization as the expected bulk damage in pixel sensors comes from the ambient hadron (mostly pion) energy flow.

The measurements will be processed and some model of the ATLAS radiation field will be developed. The measurements will be subjected to a fit by the model (similar to [10]) with the requirements that

The radial dependence can be parametrized as a polynomial with an inverse powers terms included, e.g. as in Eq. 3 and the radial function can be fitted to ATLAS radiation monitors' data points

Layer-2 of the ATLAS pixel detector is equipped with standard ATLAS radiation probes. The $_{1MeV\,eq}$ measured by radiation probes on Layer-2 should be compared with the results of fits of I/V (in A/cm^3) vs $\int L\,dt$ (in pb^{-1}) which are used to recalculate the $_{1MeV\,eq}$ based on the known current related damage rate and the radiation to luminosity rate R_{dose} discussed in the subsection below. The difference between the two measurements will give us an estimate of the systematic uncertainty of the method based on leakage currents.

2.3. Expected Precision of the HVPP4 Current Measurements

We assume that the most critical aspect of the analysis is the linear fit using Eq. 1. Measurement statistics will determine the fit errors of the slope parameter. Therefore the predictions will involve

the HVPP4 precision on current measurements which should be taken as a systematic uncertainty. We expect that the precision (HVPP4) of the current measurement board will be some fixed level of current uncertainty determined by the circuitry of the board.

the number of points, e.g. the number of data runs or smaller accessible data periods with corresponding current measurements averaged over every data run or period.

the uncertainty on the luminosity values provided by the ATLAS luminosity group. This factor determines the period defined by the ATLAS Central DAQ (e.g. run or run section) when the most reliable L measurements made by the ATLAS luminosity monitors are available. After several years of data taking the uncertainty on L will reach (L) 6% if it follows the experience of other experiments (H1, CDF, D). During the first three years we expect the uncertainty to be larger, (L) 10%.

Another contribution to the uncertainty is due to the error on , see Eq. (2).

CDF [11][12] used a more conservative estimate:

$$(3.0 \quad 0.6) \quad 10^{17}\ \mathrm{A/cm}\ ;$$

From this we expect an uncertainty ( ) 20%.

In conclusion, the HVPP4 current measurement precision will be determined by some fixed uncertainty to be derived from engineering specifications. The uncertainty should comply with dominating uncertainties coming on L and .

2.4. ATLAS MC Simulation Results: Expected Flux and Fluence

The radiation fields in the ATLAS Detector have been predicted with a full MC simulation [13]. The fluence dependence as a function of radius has been parametrized as in Eq. 3,

$$_{1MeV\,eq} = (a_2 \quad r^{2} + a_1 \quad r^{1})/1000\,\mathrm{fb}^{1} \qquad (3)$$

The polynomial coefficients are shown in Table III.

Table III Fluence parametrization: the polynomial coefficients for ATLAS Pixel Detector z 0.0 cm position along the beam axis.

Mean z, cm	a_2	a_1
0	$4.93 \quad 10^{16}$	$0.25 \quad 10^{16}$
The numbers normalized to $\int L\,dt = 1000\,\mathrm{fb}^{1}$		

The model expressed by Eq. 3 assumes that the MC simulation results when the z-coordinate is set as $z = 0.0$ cm is good for the whole barrel region of the Pixel Detector. Moreover as the worst case scenario for the pixel disk layers, the model is recommended [13] to be extended over the whole $z \in$ (650 mm; +650 mm) range between end cap disk 3 layers. For $z \in$ (650 mm; +650 mm) the model conjectures a cylindrical symmetry of the fluence field

$$_{1MeV\,eq}(r;\ ;z) \quad _{1MeV\,eq}(r)$$

The next caveat should be added here: a possible LHC beam offset w.r.t. ATLAS geodetic center will break the cylindrical symmetry.

The fluence in the Pixel Detector area with z = 0.0 cm simulation assumption [13] for an integrated luminosity $\int L\,dt$ = 10 and 100 fb^{-1} is shown in Fig. 1.

Figure 1: The fluence for $\int L\,dt = 10; 100;$ of collisions, predicted in the Pixel Detector region for z = 0.0 cm [13]. The r-positions for Layer-0,-1,-2 are shown with vertical lines.

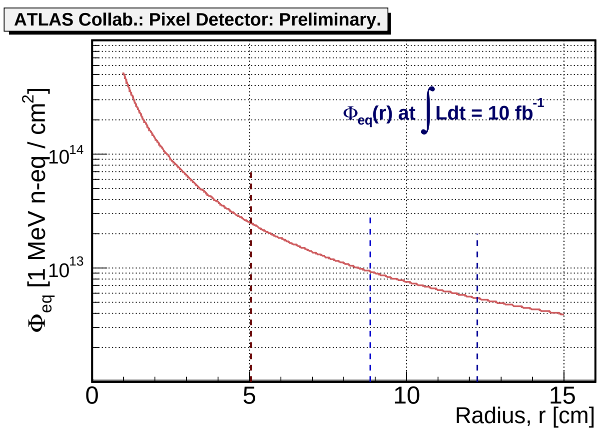

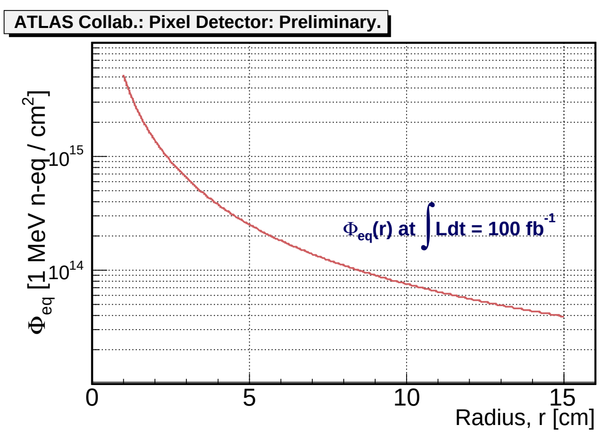

2.5. Barrel Layers: Preliminary Estimates of the Slopes of I/V versus $\int L\,dt$

The slopes for the barrel area Layer-0, Layer-1 and Layer-2 are different:

$$slope_{L0} > slope_{L1} > slope_{L2}$$

We assume from Eq. (2). The slopes differ because the fluence depends strongly upon the radius as is shown in the previous subsection, $\Phi_{1MeV\,eq}(r)$. We will have experimental measurements from the standard ATLAS probes [8] installed at Layer-2, as well as the measurements to come from the other points instrumented by standard ATLAS radiation monitors [8]. We can calibrate the parametrization model expressed by Eq. (3) and shown in Table III, which was based on MC predictions using experimental points.

Another conjecture we make here is that all modules on the same Iseg channel draw the same current. At real experimental conditions the modules will be drawing different currents due to variations of temperature and other running conditions.

The most recent temperature data allow us to apply the temperature corrections under realistic conditions. Shown in Fig. 2 are the leakage current readings at maximum temperatures reached during the cosmic run of Fall 2008. Table IV shows fluences and leakage current values for several luminosities and for Layer-0, Layer-1 and Layer-2 at the maximum temperatures specified in the table.

Table IV Currents predicted by MC at the maximum temperatures recorded during the Fall 2008 cosmic run.

ATLAS Pixel Layer-0: t_{max} = 0.8 C		
$\int L\,dt$, fb^{-1}	$\Phi_{1MeV\,eq}$, cm^{-2}	I_{Leak}, μA
0.100	2.428193e+11	3.325354e-01
1.000	2.428193e+12	3.325354e+00
10.000	2.428193e+13	3.325354e+01
100.000	2.428193e+14	3.325354e+02
1000.000	2.428193e+15	3.325354e+03
1400.000	3.399471e+15	4.655496e+03
1500.000	3.642290e+15	4.988031e+03
ATLAS Pixel Layer-1: t_{max} = +1.6 C		
$\int L\,dt$, fb^{-1}	$\Phi_{1MeV\,eq}$, cm^{-2}	I_{Leak}, μA
0.100	9.119346e+10	1.597900e-01
1.000	9.119346e+11	1.597900e+00
10.000	9.119346e+12	1.597900e+01
100.000	9.119346e+13	1.597900e+02
1000.000	9.119346e+14	1.597900e+03
1400.000	1.276708e+15	2.237059e+03
1500.000	1.367902e+15	2.396849e+03
ATLAS Pixel Layer-2: t_{max} = +7.1 C		
$\int L\,dt$, fb^{-1}	$\Phi_{1MeV\,eq}$, cm^{-2}	I_{Leak}, μA
0.100	5.326114e+10	1.616612e-01
1.000	5.326114e+11	1.616612e+00
10.000	5.326114e+12	1.616612e+01
100.000	5.326114e+13	1.616612e+02
1000.000	5.326114e+14	1.616612e+03
1400.000	7.456560e+14	2.263257e+03
1500.000	7.989171e+14	2.424918e+03

Fig. 3 shows the predicted leakage currents up to 1500 fb^{-1} for the minimum temperatures reached during the Fall 2008 cosmic run. We expect that these

Figure 2: The expected currents at maximum operational temperature values reached in the Fall 2008 Cosmic Run by the Pixel Detector barrel Layer-0, Layer-1 and Layer-2 versus the integrated luminosity in two ranges: $\int L\,dt \in (10\,pb^{-1}; 10\,fb^{-1})$ (upper plot) and $\int L\,dt \in (10\,fb^{-1}; 1500\,fb^{-1})$ (lower plot). The different slopes due to different fluences through Layer-0, Layer-1 and Layer-2 are seen in log-scaled coordinates as the offsets between lines. The higher operational temperature, 7.1 °C for outer Layer-2, raises the current to values similar to those in Layer-1 which is kept at temperature 1.6 °C.

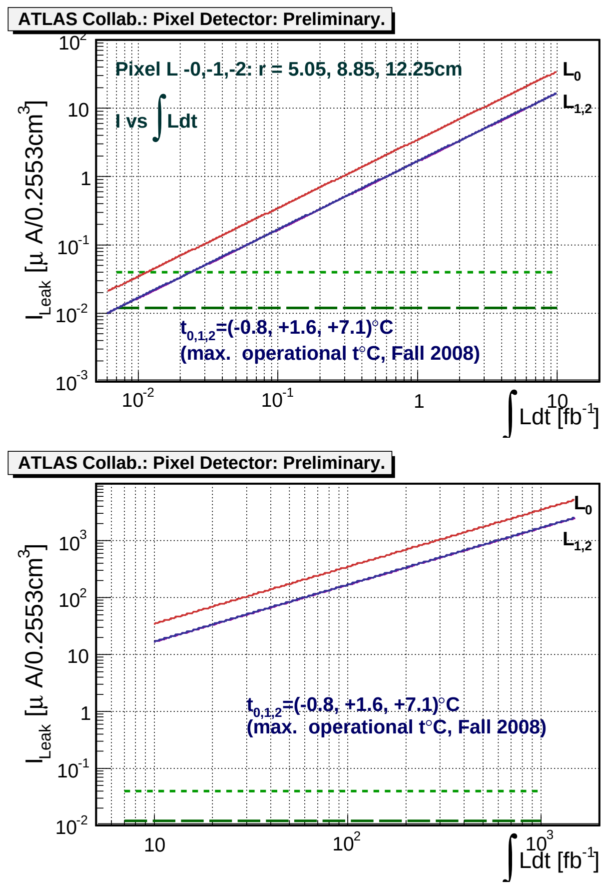

Figure 3: The expected currents at minimal operational temperature values reached in Fall 2008 Cosmic Run by the Pixel Detector barrel Layer-0, Layer-1 and Layer-2 versus the integrated luminosity in two ranges $\int L\,dt \in (10\,pb^{-1}; 10\,fb^{-1})$ (upper plot) and $\int L\,dt \in (10\,fb^{-1}; 1500\,fb^{-1})$ (lower plot). Two levels of sensitivity of the proposed Current Measurement Board, 0.01 μA (optimistic) and 0.04 μA (realistic), are shown as dashed green lines. The different slopes due to different fluences through Layer-0, Layer-1, and Layer-2 are seen in logarithm-scaled coordinates as the offsets between lines.

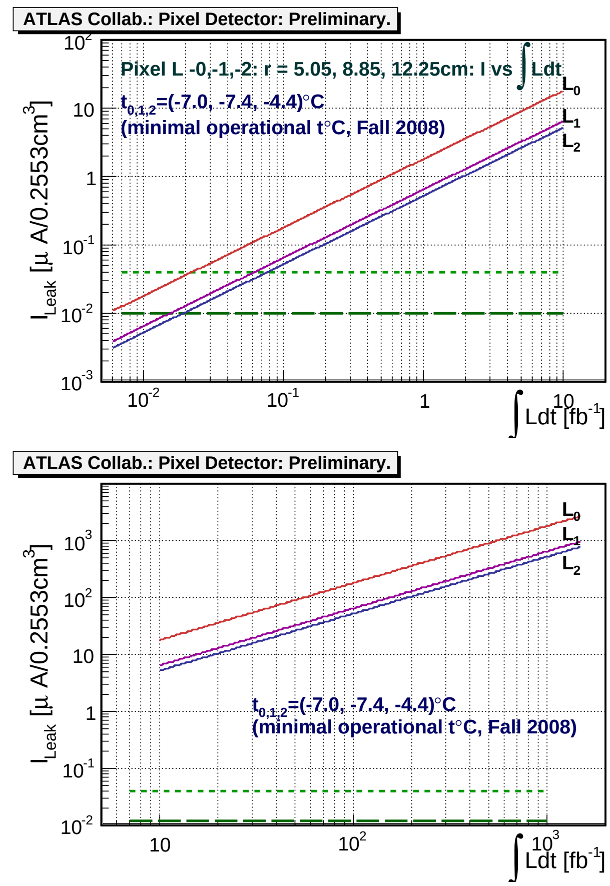

are close to realistic operational conditions. The plots also show two levels of sensitivity of the current measurement board: case 1, 0.01 μA (optimistic expectation) and case 2, 0.04 μA (realistic expectation). The sensitivity level is a crucial technical specification for the HVPP4 Current Measurement Board. Table V shows fluences and leakage current values for several luminosities and for Layer-0, Layer-1 and Layer-2 at the minimum temperatures specified in the table. Based on the values presented in the table, one can evaluate the ratio between the minimum (at $\int L\,dt \approx 100\,pb^{-1}$) and maximum (at $\int L\,dt \approx 1500\,pb^{-1}$) expected currents to be $\approx 0.5 \cdot 10^5$. The required dynamic range of leakage currents to be processed is technically challenging.

2.6. Disk Layers: Preliminary Estimates of the Slopes of I/V versus $\int L\,dt$

In previous sections our estimates and considerations are focused on the barrel layers. Following a description in [3] eight disk sectors are mounted on a 312 mm diameter carbon composite disk support ring, forming a disk. There are three disks in each of the two end-caps. Three modules are mounted on each side of the sector, with the long dimension of

Table V Currents predicted at the minimum temperatures recorded during Fall 2008 cosmic run.

ATLAS Pixel Layer-0: $t_{min} = -7.0\,^{\circ}C$		
$\int L\,dt$, fb^{-1}	$\Phi_{1MeV\,eq}$, cm^{-2}	I_{Leak}, μA
0.100	2.428193e+11	1.724755e-01
1.000	2.428193e+12	1.724755e+00
10.000	2.428193e+13	1.724755e+01
100.000	2.428193e+14	1.724755e+02
1000.000	2.428193e+15	1.724755e+03
1400.000	3.399471e+15	2.414657e+03
1500.000	3.642290e+15	2.587133e+03

ATLAS Pixel Layer-1: $t_{min} = -7.4\,^{\circ}C$		
$\int L\,dt$, fb^{-1}	$\Phi_{1MeV\,eq}$, cm^{-2}	I_{Leak}, μA
0.100	9.119346e+10	6.202588e-02
1.000	9.119346e+11	6.202588e-01
10.000	9.119346e+12	6.202588e+00
100.000	9.119346e+13	6.202588e+01
1000.000	9.119346e+14	6.202588e+02
1400.000	1.276708e+15	8.683623e+02
1500.000	1.367902e+15	9.303882e+02

ATLAS Pixel Layer-2: $t_{min} = -4.4\,^{\circ}C$		
$\int L\,dt$, fb^{-1}	$\Phi_{1MeV\,eq}$, cm^{-2}	I_{Leak}, μA
0.100	5.326114e+10	4.999913e-02
1.000	5.326114e+11	4.999913e-01
10.000	5.326114e+12	4.999913e+00
100.000	5.326114e+13	4.999913e+01
1000.000	5.326114e+14	4.999913e+02
1400.000	7.456560e+14	6.999878e+02
1500.000	7.989171e+14	7.499870e+02

the module in the radial direction. The three modules on the back side of the sector are rotated 7.5° with respect to the modules on the front side, making the overlapping to provide a full acceptance in ϕ (or pseudo-rapidity η). Each disk has on back and front sides $2 \times 24 = 48$ modules. Each end cap comprises $3 \times 48 = 144$ modules with a total of $2 \times 144 = 288$ modules for both end caps.

The radius of the module centers is approximately $R^{center}_{disk\,module} \approx 119\,mm$. The inner radius of the active area of the pixel modules $R^{inner}_{disk\,module} \approx 89\,mm$. Please see the details in [3].

We follow the general conjecture made in [13] about weak z-dependence of the fluence in the Pixel Detector area especially in the barrel region. We extrapolate this approach to the endcap area taking the “worst case scenario”. Thenceforth to estimate the fluence through disk modules we should integrate the dependence in Eq. 3 over radial area of $(88.88; 149.6)\,mm$ and take an average. Please see the Eq. 4.

$$<\Phi^{disk}_{1MeV\,eq}> \propto \int_{R_{out}}^{R_{inn}} d\phi \; r\,dr \; \Phi_{1MeV\,eq}(r) \quad (4)$$

Using the same numbers from Ian Dawson's recent update [13] on fluence in ATLAS Pixel Detector area including disks (see also a discussion in Section 2.4), $R_{inn} = 8.88\,cm$; $R_{out} = 14.96\,cm$; and $a_2 = 4.93 \times 10^{+16}$; $a_1 = 0.25 \times 10^{16}$, the averaged over disk module fluence per $1000\,fb^{-1}$ can be calculated to be

$$<\Phi^{disk:sens.}_{1MeV\,eq}>_{1000\,fb^{-1}} \approx 5.64 \times 10^{14}\,cm^{-2}$$

Below the Table VI shows the fluences and leakage currents values for several luminosities and for Disk Layer at the minimum and maximum Fall 2008 temperatures specified in the table. Again here as for the barrel case we assume that all modules are drawing the currents of the same value.

Table VI Currents in disk layer predicted at the minimum and maximum temperatures recorded during Fall 2008 cosmic run.

ATLAS Pixel Disk Layers: $t_{min} = -7.3\,^{\circ}C$		
$\int L\,dt$, fb^{-1}	$\Phi_{1MeV\,eq}$, cm^{-2}	I_{Leak}, μA
0.100	5.645341e+10	3.881622e-02
1.000	5.645341e+11	3.881622e-01
10.000	5.645341e+12	3.881622e+00
100.000	5.645341e+13	3.881622e+01
1000.000	5.645341e+14	3.881622e+02
1400.000	7.903477e+14	5.434271e+02
1500.000	8.468011e+14	5.822433e+02

ATLAS Pixel Disk Layers: $t_{max} = -3.4\,^{\circ}C$		
$\int L\,dt$, fb^{-1}	$\Phi_{1MeV\,eq}$, cm^{-2}	I_{Leak}, μA
0.100	5.645341e+10	5.891448e-02
1.000	5.645341e+11	5.891448e-01
10.000	5.645341e+12	5.891448e+00
100.000	5.645341e+13	5.891448e+01
1000.000	5.645341e+14	5.891448e+02
1400.000	7.903477e+14	8.248027e+02
1500.000	8.468011e+14	8.837172e+02

The temperatures at disk layer areas have been held lower than for outer barrel layers Layer-1 and Layer-2. The fluences at disk area shown in Table VI are similar to the ones at barrel Layer-2, see Table V. Thus the leakage currents in disk layer at its minimal temperature are similar to the ones of barrel Layer-2, see Table V, but somewhat lower at its maximum temperature reached during Fall 2008. That said we conjecture that the specified range of the currents to be sensed by the Current Measurement Board is in compliance with the currents to be drawn by the disk modules given the temperatures observed during Fall 2008 cosmic runs.

3. Current Measurement Board

The present HVPP4 System serves as a fan-out point for the bias voltages delivered by Type II boards from Iseg power supplies to 1744 pixel modules. The current measurement function of HVPP4 system is technically implemented by Current Measurement Board mounted on every Type II fan-out board.

The analog current measurements are further digitized by the ATLAS standard 64-channel ELMB board [14][15] and sent via CAN bus to DCS database (see also [2]). The ADC serving every of the ELMB channels can be con gured for a full-scale measurement of the voltage coming from Current Measurement Board in the next 5 ranges [15]:

V_{input} 2 (0:;25) mV, V_{input} 2 (0:;100) mV, ...

...V_{input} 2 (0:;1) V, V_{input} 2 (0:;2:5) V, ...

V_{input} 2 (0:;5) V.

the 16 bits of ADC provides the resolution of (0;65535) [14] for an every of above speci ed ranges.

The speci cation for a range of currents to be measured with the board comes from our estimates of currents for the expected integrated luminosities to be delivered by LHC, see Fig. 2 and Fig. 3.

(0:04 A ; 2 mA) with a dynamical range of 0:5 10^5

the output voltage of the board should lie within (0:; 5)V_{DC} to comply the digital board ELMB speci cations outlined above.

the circuit of the Current Measurement Board is a current to frequency converter which in turn is optically coupled to a frequency to voltage converter

{ the pairs of channels are isolated from each other and

the board is a multi-layer PCB holding 13 current measurement circuits and providing the current measurements for 13 channels (pixel modules)

the pairs of channels are isolated from each other and from the pixel module readout system

The con guration will consist of several VME crates:

One VME crate lled with 9 Type II boards

{ Current Measurement Board mounted on every Type II board, 9 boards per VME crate

{ 13 channels per Current Measurement Board: 9 13 channels per crate

{ 2 ELMB boards to digitize and send data over CAN bus to ATLAS DCS database

In total the HVPP4 system consists of 16 VME crates to serve 16 9 13 = 1872 channels well enough for 1744 modules

Recently the pre-prototype of the Current Measurement Board was laid out and produced. The board has been tested with calibrated current source from Keithley, with real ATLAS tile and chip sensors biased to the appropriate voltage at 20 C. The responses of the pre-prototype board are shown at plots, see Fig. 4. The nice linearity has been observed.

4. Summary

We have described the principles of radiation damage monitoring using the current measurements to be provided by the circuits of the HVPP4 system. The dependence of the leakage current with respect to the integrated luminosity at several temperature scenarios has been presented. Based on the analysis we have evaluated the sensitivity speci cations for the Current Measurement Board to be a crucial subsystem of HVPP4. The pre-prototype of the Current Measurement Board has been developed, produced and tested with real ATLAS sensors and at SR1 area in ATLAS pit. A regular linear behavior of the response has been obtained with real ATLAS sensors at 20 C and with a calibrated current source.

Acknowledgments

The authors are grateful to Dr. Maurice Garcia-Sciveres (LBNL) and Rusty Boyd (University of Oklahoma) for their contributions and continuous support of the project.

References

[1] R. Boyd, "ATLAS Pixel PP4 HV Design. Speci cation for construction and use of Patch Panel 4 High Voltage Services", CERN EDMS Document, Number: ATL-IP-ER-0017, EDMS Id: 772658, 2006-09-11, CERN.

[2] G. Aad, "ATLAS pixel detector electronics and sensors," JINST 3, P07007 (2008).

[3] G. Aad et al. [ATLAS Pixel Collaboration], "The ATLAS pixel detector mechanics and services", to be submitted to Journal of Instrumentation, 2008 JINST

Figure 4: The response of a pre-prototype current measurement board. The upper plot shows the response of the board to the calibrated current supplied by Keithley power source. The middle plot includes also the current drawn by biased ATLAS tile and chip sensors. The lowest plot is a result of the tests made at SR1 ATLAS pit area using Keithley power source feeding currents into the measurement board, ELMB digital board processing analog output of the measurement board and the PVSS software reading out and formatting the digital data.

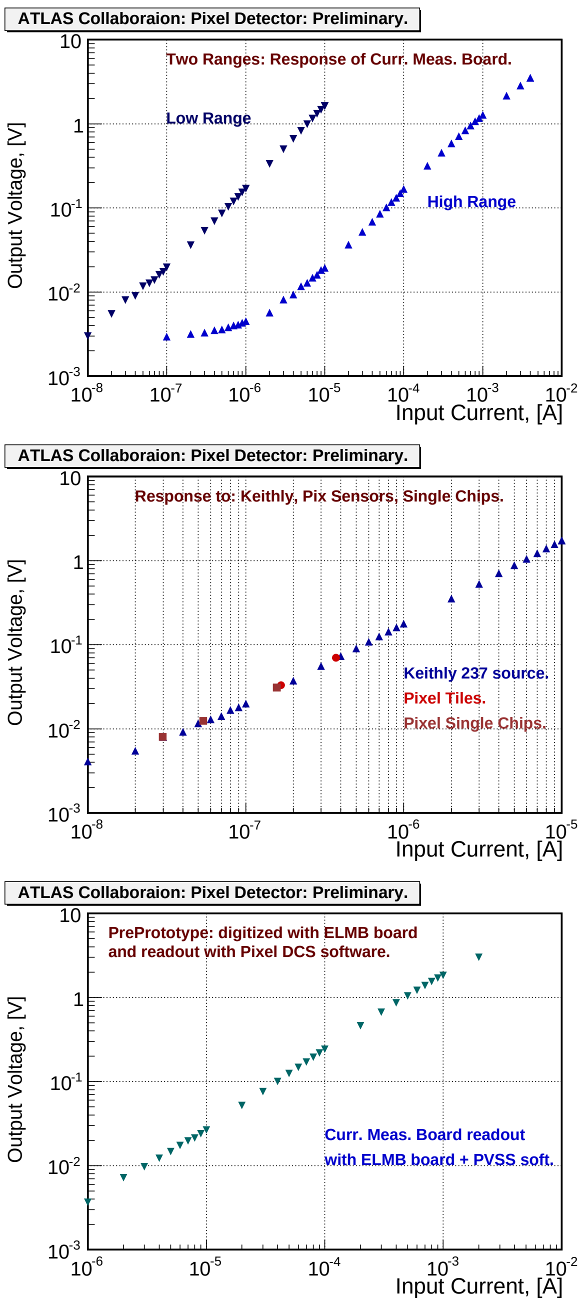

[4] M. Garcia-Sciveres [ATLAS Collaboration], "Post-installation status of the ATLAS pixel detector," JINST 4, P03021 (2009).

[5] T. Golling, Nucl. Instrum. Meth. A 604, 293 (2009).

[6] E. Galyaev, "Results from the Commissioning of the ATLAS Pixel Detector with Cosmic data,", talk made on behalf of the ATLAS Collaboration at the DPF-2009 Conference, Detroit, MI, July 27-31, 2009; to be published in the Proceedings, arXiv:0910.0847 [physics.ins-det].

[7] iseg Spezialelektronik GmbH, Bautzner Landstr. 23, D-01454 Radeberg/Rossendorf, http://www.iseg-hv.de, High Voltage Power Supply EHQ F607n-F, Operators Manual.

[8] J. Hartert, J. Bronner, V. Cindro, A. Gorisek, G. Kramberger, I. Mandic and M. Mikuz, "The ATLAS radiation dose measurement system and its extension to SLHC experiments", CERN-2008-008, 2008. 5pp.
Talk made at a Topical Workshop On Electronics For Particle Physics "TWEPP 2008", 15-19 Sep 2008, Naxos, Greece. Published in the Proceedings "Naxos 2008, Electronics for particle physics", pp. 269-273

[9] M. Moll, E. Fretwurst and G. Lindstrom [CERN-ROSE/RD48 Collaboration], Nucl. Instrum. Meth. A 426, 87 (1999).

[10] S. D'Auria, J. A. Hocker, S. McGimpsey, K. Kordas, R. J. Tesarek and S. Worm, Nucl. Instrum. Meth. A 513, 89 (2003). See also CDF public note CDF/PUB/PUBLIC/6753.

[11] S. Worm [CDF Collaboration], Nucl. Instrum. Meth. A 549, 126 (2005).

[12] Steven Worm, Life Expectancy of the Run II Silicon, CDF public note, CDF/PUB/SEC_VTX/6673

[13] Atlas Radiation Background Task Force Summary Document, "Estimation of Radiation Background, Impact on Detectors, Activation and Shielding Optimization in ATLAS", ATLAS Note, ATL-GEN-2005-001, 13 January 2005. See also an update in a recent talk
Ian Dawson, http://indico.cern.ch ...
.../conferenceDisplay.py?confId=52704

[14] J. R. Cook (james.cook@cern.ch) & G. Thomas (geraldine.thomas@cern.ch), "ELMB128 Documentation", https://edms.cern.ch/file/684947 ...
.../LAST_RELEASED/ElmbUserGuide.pdf

[15] Henk Boterenbrood, "CANopen Application Software for the ELMB128 (Embedded Local Monitor Board)", Version 2.2, 13 January 2005, NIKHEF, Amsterdam,
http://www.nikhef.nl/pub/departments ...
... /ct/po/html/ELMB128/ELMB22.pdf,